MicroRNA-122, a Tumor Suppressor MicroRNA that Regulates Intrahepatic Metastasis of Hepatocellular Carcinoma

Wei-Chih Tsai,[1]* Paul Wei-Che Hsu,[5]* Tsung-Ching Lai,[7]* Gar-Yang Chau,[8] Ching-Wen Lin,[1] Chun-Ming Chen,[1] Chien-Der Lin,[2] Yu-Lun Liao,[1] Jui-Ling Wang,[7] Yat-Pang Chau,[3] Ming-Ta Hsu,[4] Michael Hsiao,[7]* Hsien-Da Huang,[5,6]* and Ann-Ping Tsou[1,7]*

MicroRNAs (miRNAs), which are inhibitors of gene expression, participate in diverse biological functions and in carcinogenesis. In this study, we show that liver-specific *microRNA-122 (miR-122*) is significantly down-regulated in liver cancers with intrahepatic metastastasis and negatively regulates tumorigenesis. Restoration of *miR-122* in metastatic Mahlavu and SK-HEP-1 cells significantly reduced *in vitro* migration, invasion, and anchorage-independent growth as well as *in vivo* tumorigenesis, angiogenesis, and intrahepatic metastasis in an orthotopic liver cancer model. Because an inverse expression pattern is often present between an miRNA and its target genes, we used a computational approach and identified multiple *miR-122* candidate target genes from two independent expression microarray datasets. Thirty-two target genes were empirically verified, and this group of genes was enriched with genes regulating cell movement, cell morphology, cell-cell signaling, and transcription. We further showed that one of the *miR-122* targets, ADAM17 (a disintegrin and metalloprotease 17) is involved in metastasis. Silencing of ADAM17 resulted in a dramatic reduction of *in vitro* migration, invasion, *in vivo* tumorigenesis, angiogenesis, and local invasion in the livers of nude mice, which is similar to that which occurs with the restoration of *miR-122*. *Conclusion:* Our study suggests that *miR-122*, a tumor suppressor microRNA affecting hepatocellular carcinoma intrahepatic metastasis by angiogenesis suppression, exerts some of its action via regulation of ADAM17. Restoration of *miR-122* has a far-reaching effect on the cell. Using the concomitant down-regulation of its targets, including ADAM17, a rational therapeutic strategy based on *miR-122* may prove to be beneficial for patients with hepatocellular carcinoma. (HEPATOLOGY 2009;49:1571-1582.)

Since their discovery in *Caenorhabditis elegans* as important regulators of development timing,[1] endogenous small hairpin microRNAs (miRNAs) have been found to have a broad impact on vertebrates and invertebrates by regulating gene activities through translational repression[2] or posttranscription suppression.[3-5] Rapid advances in the molecular characterization of miRNAs has not only revealed their physiological functions but also uncovered abnormal patterns of miRNA expression linked to many disease states including cancer.[6,7] Hepatocellular carcinoma (HCC) is one of the most common human malignancies; this disease shows exceptional

Abbreviations: ADAM17, a disintegrin and metalloprotease 17; HCC, hepatocellular carcinoma; miRNA, microRNA; miR-122, microRNA-122; shRNA, small-hairpin interfering RNA; 3′ UTR, 3′ untranslated region; T1, stage I HCC; T3, stage III HCC.

From the [1]Department of Biotechnology and Laboratory Science in Medicine, [2]Institute of Bioinformatics, [3]Anatomy and Cell Biology, and [4]Biochemistry and Molecular Biology, National Yang-Ming University, Taipei, Taiwan (Republic of China [ROC]); [5]Institute of Bioinformatics and [6]Department of Biological Science and Technology, National Chiao Tung University, Hsin-Chu, Taiwan (ROC); [7]Genomics Research Center, Academic Sinica, Nankang, Taipei, Taiwan (ROC); [8]Department of Surgery, Taipei Veterans General Hospital, Taipei, Taiwan (ROC).

Received August 12, 2008; accepted December 13, 2008.

Supported in part by the grants NSC 96-3112-B-010-017 and NSC 95-2752-B-010-002-PAE from the National Science Council to A.P.T., NSC 95-2311-B-009-004-MY3 to H.D.H., and a grant from the Ministry of Education, Aim for the Top University Plan to A.P.T. and Y.P.C.

**These authors contributed equally to this work.*

heterogeneity in cause and outcome. It is especially prevalent among Asian populations. Despite successful local therapies such as surgery or transcatheter arterial chemoembolization, patients with HCC develop a high rate of recurrence due to local invasion and intrahepatic metastasis. Liver cancer is a complex disease involving epigenetic instability, chromosomal instability,[8] and expression abnormalities of both coding[9,10] and noncoding genes; the latter includes miRNAs.[11-14] Profiling of miRNA expression has identified signatures associated with HCC formation and progression that are potential cancer biomarkers. One such metastasis signature, consisting of 20 miRNAs, has been recognized as an independent predictor of survival.[12] Deregulation of these 20 miRNAs in metastatic HCC implies that altered expression of their pertinent target genes may contribute to the development of metastasis or to recurrence. *MicroRNA-122* (*miR-122*) is a member of this metastasis signature.

Recent work on tissue-specific miRNAs has demonstrated their participation in tissue specification and cell lineage decisions.[15,16] *MiR-122* is a liver-specific miRNA known to modulate lipid metabolism,[4,17] hepatitis C virus replication,[18] and antiapoptosis.[19] Persistent expression of *miR-122* has been detected during liver specialization into adult liver,[20] yet *miR-122* is down-regulated in HCC.[21] Currently, only a handful of confirmed target genes of *miR-122* have been reported;[4,17,20,22] hence, involvement of *miR-122* as an effector of hepatocyte differentiation remains to be established.

In this study, we demonstrated that the loss of *miR-122* expression in the intrahepatic metastasis of liver tumors is highly significant. We determined a functional role for *miR-122* in liver tumor progression using both *in vitro* and *in vivo* models. Furthermore, we applied a bioinformatics-based computational prediction approach to investigate the *miR-122* targets based on two microarray datasets where *miR-122* is significantly down-regulated, one with local invasion of HCC and the other involving antagomir-122–treated mouse livers. Finally, we carried out target verification by 3′ untranslated region (3′UTR) reporter assay and expression analysis. Based on involvement in regulating cell adhesion, migration, and metastasis, a disintegrin and metalloprotease 17 (ADAM17), an empirically verified target gene of *miR-122*, was chosen for in-depth investigation.

Patients and Methods

Cell Lines and Human Liver Tissues. The human HCC cell lines Mahlavu, HuH-7, and SK-HEP-1 as well as the human embryonic kidney cell line HEK293T were cultured as described.[23] Paired samples of tumor/nontumorous liver tissues were obtained from patients who had undergone primary HCC curative hepatic resection at Taipei Veterans General Hospital, Taiwan. The study was approved by the Committee for the Conduct of Human Research, and patient informed consent was obtained. This study consisted of 48 HCC samples from two tumor-node-metastasis (TNM) stages, stage I (T1, n = 25) and stage III (T3, n = 23), according to the American Joint Committee on Cancer 6th edition TNM classification. Immediately after surgical resection, all tissues were snap-frozen in liquid nitrogen and stored at −80°C.

Gene Expression Analysis. Expression analysis of *miR-122* was done by low stringency northern blotting and TaqMan MicroRNA Assay (Applied Biosystems, Foster City, CA). RNA (20 μg) was separated on a 15% denaturing polyacrylamide gel, transferred to Hybond-N$^+$ membrane (Amersham Bioscience, Piscataway, NJ), and hybridized with a [γ-^{32}P]-labeled 5′-ACAAACACCATTGTCACACTCCA-3′ probe. The most stringent wash was carried out using 2× standard sodium citrate, 0.5% sodium, dodecyl sulfate at 42°C before autoradiography. The same blot was reprobed for *U6 snRNA*l. TaqMan MicroRNA Assay, a quantitative stem-loop polymerase chain reaction was performed according to the manufacturer's specifications with *U6* RNA as an internal control. Expression of *pri-miR-122* was detected byRT-PCRusingtheprimers5′-GCTCTTCCCATTGCTCAAGATG-3′ and 5′-GTATGTAACAACAGCATGTG-3′. Expression levels of *miR-122* target genes were also examined by reverse transcription polymerase chain reaction (RT-PCR) (primer sequences in Supporting Table 6).

Plasmid Constructs. A partial human *pri-miR-122* gene (a 562–base pair complementary DNA fragment encompassing 54,269,034 base pairs to 54,269,595 base

Address reprint requests to: Ann-Ping Tsou, D.Sc., Department of Biotechnology and Laboratory Science in Medicine, National Yang-Ming University, Taipei 112, Taiwan, Republic of China, E-mail: aptsou@ym.edu.tw; fax: (886)-2-28264092.

Published online in Wiley InterScience (www.interscience.wiley.com).

DOI 10.1002/hep.22806

Potential conflict of interest: Nothing to report.

Additional Supporting Information may be found in the online version of this article.

pairs of 18q21.31, University of California Santa Cruz Genome Browser) was subcloned into the lentiviral expression vector, pPGK-GFP (National RNAi Core Facility, Academia Sinica, Taiwan) in place of GFP and called pPGK-122. pPGK-GFP, a positive control for the lentiviral infection, contains necessary *cis*-elements for packaging, reverse transcription and integration. PGK stands for the human phosphoglycerate kinase promoter sequences. pPGK-122 was used to make lentiviruses expressing *miR-122* (lenti-122). A *miR-122* seed-region (5′-GGAGTGTG-3′ to 5′-ATGACTGA-3′) mutant (lenti-122M) was constructed using a QuickChange Site-Directed Mutagenesis Kit (Stratagene, La Jolla, CA).

Ectopic Expression of miR-122. Stable HCC cell cultures expressing *miR-122* were generated by coinfecting HCC cells with lenti-122 and short hairpin Luciferase (shLuc) at 100:1 ratio using 8 μg/mL protamine sulfate for 24 hours and puromycin (2 μg/mL) selection for 3-5 days. The shLuc targeting the luciferase gene provides the puromycin resistance. Expression of mature *miR-122* was confirmed by northern blotting.

Prediction of miR-122 Targets Among Differentially Expressed Genes. For *miR-122* target prediction, we applied miRanda[24] to energetically detect the most probable targets against the 3′UTR among all human and mouse coding genes (BioMart from the Ensembl database[25]). The miRNA/target duplexes with miRanda scores greater than 120 and minimum free energy values less than −10 kcal/mol were identified as *miR-122* target sites. The analysis strategy is presented in Supporting Table 2.

3′ UTR Reporter Assay. The 3′UTR fragments of the candidate target genes were subcloned into the Xba1 site downstream of the luciferase gene in pGL3-Control Vector (Promega, Madison, WI). Under the control of SV40 promoter and enhancer, pGL3-Control Vector expresses strong luciferase activity in many types of mammalian cells. The negative controls were lenti-122M and lenti-GFP. HEK293T cells were infected with lenti-GFP and lenti-122 or lenti-122M for 24 hours. Cells were then seeded into 24-well plates and cotransfected with 0.5 μg of the respective pGL3-3′UTR construct and 0.05 μg of the pRL-TK vector (Promega) using jetPEI (Polyplus-Transfection, France). pRL-TK vector was used as an internal control reporter. After 48 hours, luciferase activity was measured using the Dual-Luciferase Reporter Assay System Kit (Promega). The effect of *miR-122* was expressed relative to the average value from cells infected with lenti-GFP virus. A mutant of the single *miR-122* binding site (5′-ACACUCCA-3′ to 5′-ACCCGCAA-3′) in the 3′UTR of ADAM17 was included. The mutagenesis primers are listed (Supporting Table 7) together with the nucleotide sequences of all the PCR cloning primers (Supporting Table 8).

RNA Interference with shADAM17. HCC cells were plated and infected with lentiviruses expressing shADAM17 or shLuc in the presence of 8 μg/mL protamine sulfate for 24 hours followed by puromycin (2 μg/mL; 48 hours) selection. RT-PCR and/or western blotting were performed to validate the knockdown efficiency. The shRNA constructs are described in Supporting Fig. 4.

Cell Migration Assay and Invasion Assay. Cells were tested for their migration and invasion abilities *in vitro* in a Minicell (Millipore) according to the methods described previously.[23]

Soft-Agar Colony Assay. Cells were seeded at 5×10^3 cells/well in a six-well plate containing 0.3% low melting temperature agarose (Sigma, St. Louis, MO). Colonies were counted after 14 days. The Integrated Morphometry analysis function of MetaMorph software (Molecular Devices, Sunnyvale, CA) was used to measure the surface areas of the colonies and derive the size of the colonies.

In Vivo Tumorigenesis Assay. Mahlavu and SK-Hep1 cells (5×10^6) infected with shLuc, lenti-122, or lenti-shADAM17 lentiviruses were implanted subcutaneously into the flanks of nude mice. Primary tumor growth was analyzed by measuring tumor length (L) and width (W), and tumor volume was calculated according to $V = 0.4 \times ab^2$ as described.[23] Orthotopical intrahepatic injection was conducted as described[27] by using 20 μL of phosphate-buffered saline containing 50% Matrigel (BD Biosciences, MA); mixed with 5×10^6 tumor cells, and slowly injected into the livers of anesthetized mice using a 27-gauge needle. Mice were sacrificed 6-7 weeks later for histopathological evaluation. The methods used for the immunohistochemical staining of anti-CD31, the evaluation of microvessel density, and the quantification of tumor size are described in Supporting Methods. Only the results using Mahlavu cells are presented. The animal studies were approved by Institutional Animal Care and Use Committee (IACUC) of National Yang Ming University.

Statistical Analyses. All data are expressed as mean ± standard deviation and compared between groups using the Student *t* test. Categorical variables were compared using the Wilcoxon Rank test. A *P* value <0.05 was considered statistically significant. $^*P < 0.05$; $^{**}P < 0.01$; $^{***}P < 0.001$.

Results

Specific Down-Regulation of miR-122 in HCC Correlates with Enhanced Transforming Activity. Recently, *miR-122* was found to be down-regulated in liver

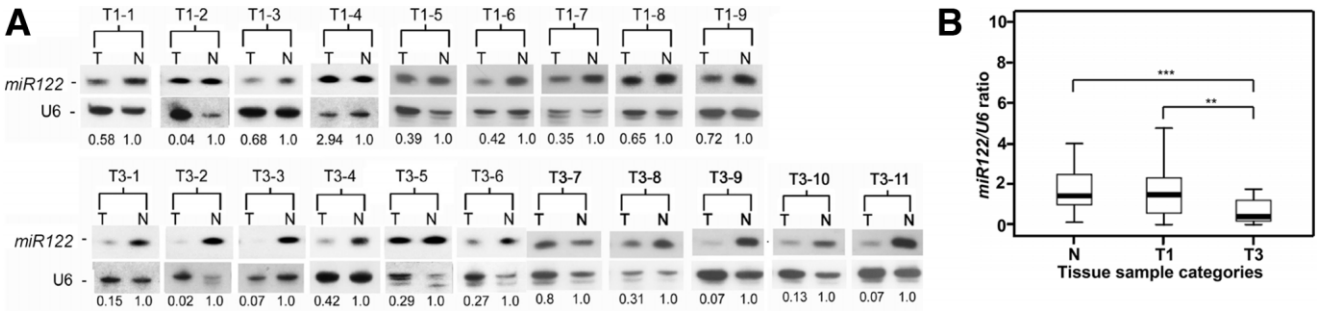

Fig. 1. Expression of *miR-122* was down-regulated in intrahepatic metastastic liver tumors. (A) Expression analysis by northern blotting. T: tumor part; N: normal adjacent tissue. The intensity of northern hybridization was retrieved using ImageQuant software. Each *miR-122* intensity value was first divided by the corresponding intensity of *U6* from the same tissue sample to adjust for sample variation. (B) Decreased *miR-122* mRNA expression was present in an additional 48 pairs of HCC samples (T1, n = 25; T3, n = 23) and demonstrated by TaqMan MicroRNA Assay. Results were normalized against the expression level of *U6* messenger RNA (mRNA) in each sample. The differences in *miR-122* expression level between tissue sample categories were analyzed by Wilcoxon rank sum test. The box plot shows the data distribution across the group classification and presents the 75th and 25th percentile (upper and lower quartile) with the median value between. T1: primary HCC, T3: intrahepatic metastasis HCC; N: an average of expression level of all 48 normal adjacent tissues. $^{**}P < 0.01$; $^{***}P < 0.001$.

tumors of human and rodents[21,22] and is considered a member of a metastasis-related microRNA signature.[12] However, the functional attributes of *miR-122* associated with liver tumor progression have not been experimentally established. To substantiate the significance of *miR-122* expression, a northern blot analysis of 20 HCC tumor pairs was conducted. Expression of *miR-122* was remarkably lower in T3 tumors with intrahepatic metastasis (Fig. 1A). Validation by quantitative stem-loop PCR showed that the expression of *miR-122* was significantly higher in the adjacent normal tissue (n = 48) and T1 tumors (n = 25). No statistically significant difference was found between T1 tumors and adjacent normal tissue. However, significant loss of *miR-122* expression was found in T3 tumors (Fig. 1B), which implies that down-regulation of *miR-122* significantly correlates with intrahepatic metastasis as reported.[12]

To explore the functional role of *miR-122* in HCC progression, ectopic overexpression of *miR-122* was established using a lentiviral vector (lenti-122). When *miR-122* was overexpressed in SK-HEP-1 or Mahlavu HCC cells (Fig. 2A), which are known to manifest invasion activity,[23] a significant reduction of cell migration and invasive activity was observed (Fig. 2B). Overexpression of *miR-122* also impaired anchorage-independent growth in soft agar, significantly reducing the number and size of the colonies (Fig. 2C). Consistent with the *in vitro* results, overexpression of *miR-122* in Mahlavu cells significantly suppressed overall tumor growth and local invasion *in vivo* (Fig. 6). Restoration of *miR-122* expression, however, did not influence HCC cell proliferation (Supporting Fig. 1). These *in vitro* and *in vivo* results imply that the gradual loss of *miR-122* over a long period of time is likely to commit hepatocytes to tumorigenesis and intrahepatic metastasis.

Identification of miR-122 Target Genes. *MiR-122* regulates multiple target genes whose combined expression is associated with the metabolism of hepatic fatty acid and cholesterol as well as HCC pathogenesis.[4,17,21] To identify putative metastasis genes that *miR-122* suppresses, we integrated various computational prediction tools to track down genes where expression was increased by >1.5-fold in T3 HCC and in antago-miR-122–treated mouse livers. The salient feature common to these two types of liver tissues is that they both have extremely low levels of endogenous *miR-122*. In addition, the genes needed to have a putative *miR-122* binding site mapped to their 3′UTR. A list of 45 most probable targets, including the known genes *SLC7A1* [20] and *ALDOA*,[4] was compiled (Table 1). A reciprocal expression pattern between *miR-122* and the candidate genes was identified by microarray (Supporting Table 1) and by RT-PCR (Supporting Fig. 2), which supports a role in their posttranscriptional suppression by *miR-122*.

Bioinformatic prediction recognized one to seven *miR-122* binding sites in the 3′UTRs of these candidate genes (Table 1, Supporting Table 3). To test whether the predicted binding sites in the target genes could mediate repression of translation by *miR-122*, the 3′UTRs were subcloned downstream of the luciferase gene in pGL3-Control. These constructs were assayed in HEK293T cells infected with lenti-*122* or a mutant *miR-122* in which the seed region has been randomly mutated (miR122-M; Fig. 3A). As shown in Fig. 3A, the reporter with the 3′UTR of *SLC7A1* showed a significantly lower luciferase activity in cells expressing *miR-122* compared to *miR122-M*. Similar responses were detected for the reporter with the 3′UTR of *AKT3*. *MiR-122* thus negatively regulates translation of these genes through the 3′UTR binding sites, and *SLC7A1* and *AKT3* are true *miR-122* target genes. A significant reduction in luciferase

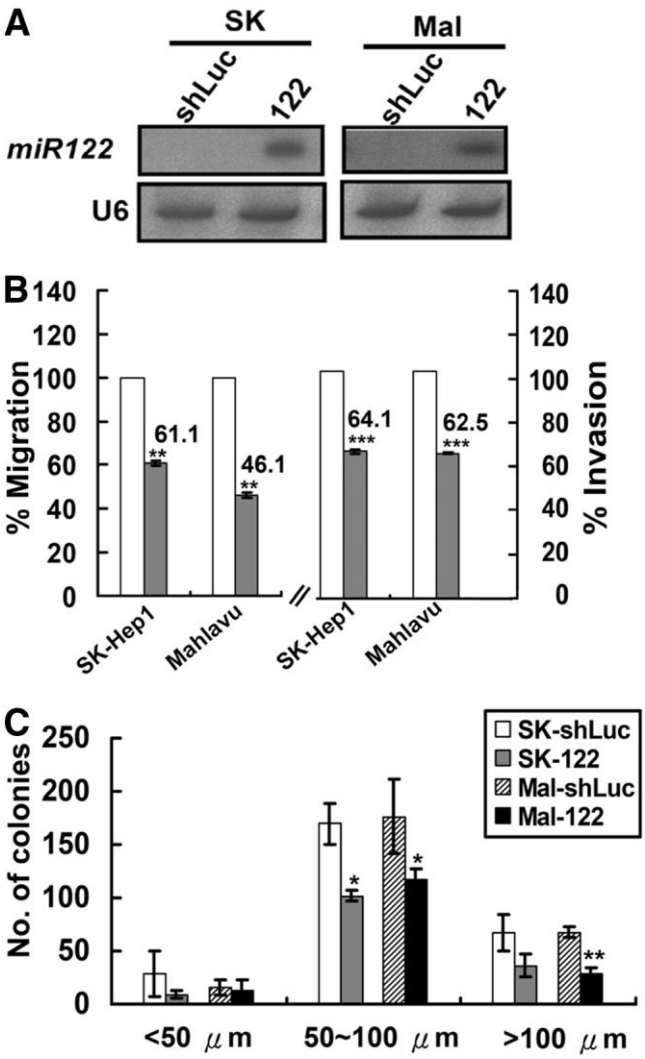

Fig. 2. *MiR-122* regulates the transforming activities of HCC cells. (A) Northern blots detected expression of mature *miR-122* from cells infected with lenti-122 lentiviruses. (B) Restoration of *miR-122* reduced cell migration and invasion. White bars, control cells infected with shLuc; gray bars, cells infected with lenti-122. (C) Anchorage-independent cell growth in soft agar of two HCC cell lines, SK-HEP-1 and Mahlavu, was reduced with *miR-122* overexpression. Two lines of HCC cells were infected with lenti-122 or control shLuc. The Integrated Morphometry analysis function of MetaMorph was used to measure the surface areas of the colonies, which were used to derive the size and distribution of the colonies. $*P < 0.05$; $**P < 0.01$; $***P < 0.001$.

activity (14%-54%) was detected with 32 of the 35 cloned reporter constructs (Fig. 3B). *STX6* (*syntaxin 6*), *SORT-1* (*sortilin-1*), and *SPRED-1* (*sprouty-related, EVH1 domain containing-1*) failed to show a significant reduction in luciferase activity. No specific repression by *miR122-M* was detected (Supporting Tables 4 and 5). These 32 genes are therefore direct targets of endogenous *miR-122*.

To uncover the biological functions of the confirmed *miR-122* targets, gene function analysis was carried out (Ingenuity Pathways Analysis 3.0; Ingenuity Systems, Redwood City, CA). Genes classified as having the molecular functions involved in "Cell Morphology" or "Cell Movement" (Supporting Fig. 3) were identified. The overlap between these two functions pinpointed three genes, *ADAM17*, *MAPK11* (*mitogen-activated protein kinase 11*), and *NCAM1* (*neural cell adhesion molecule 1*). ADAM17 plays a crucial role in the shedding of receptor ligands, such as certain epidermal growth factors (EGFs) and tumor necrosis factor alpha (TNFα), which are the major ligands for several signal transduction pathways.[28] Previous reports have shown overexpression of ADAM17 in breast cancer,[29] brain tumors,[30] and non–small cell lung cancer,[31] where the gene contributes to tumor invasiveness and metastasis. Although elevated *ADAM17* expression has been identified as a pathological feature of HCC,[32,33] its function has not been determined. Therefore, we evaluated the functional role of ADAM17 in HCC tumorigenesis and progression.

ADAM17 Is a Critical Downstream Target of miR-122. *ADAM17* has one 3′UTR high-scoring binding site. The fact that expression from the 3′UTR reporter corresponding to the parental *ADAM17* sequences (but not from one with a mutated binding sequences, *ADAM17-M*) had significantly suppressed luciferase activity in *miR-122* transfected 293T cells confirmed the authenticity of this binding site (Fig. 4B). The knockdown of ADAM17 in SK-HEP-1 and Mahlavu cells (Fig. 4C) showed significant reduction in cell migration and invasion (Fig. 4D) as well as lower anchorage-independent growth in soft agar (Fig. 4E); this is similar to the phenotype detected with *miR-122* restoration in these two lines of HCC cells (Fig. 2B,C). However, one difference from *miR-122* restoration was that shADAM17 reduced the proliferation of Mahlavu cells (Supporting Fig. 4)

Moreover, overexpression of *miR-122* or knockdown of ADAM17 brought about cell morphology changes and actin disorganization as shown by the confocal images of cells stained with the F-actin marker phalloidin (Fig. 5, Supporting Methods). Phalloidin-stained *miR-122*-Mahlavu cells showed a severe reduction of stress fibers (middle panel, Fig. 5A), which is similar to that of SK-N-SH cells treated with RhoA[14] and forskolin.[34] Surprisingly, there was an overwhelming reduction of membrane protrusions, and this was accompanied by a contracted cell shape in shADAM17-Mahlavu cells (right panel, Fig. 5A). Restoration of *miR-122* impacted on the epithelial-mesenchymal transition as shown by a reduction in vimentin, a mesenchymal marker (Fig. 5B). Cell motility requires the formation of membrane protrusions such as lamellipodia or filapodia, a process that revolves around actin dynamics under the control of Rho–guanosine

Table 1. Candidate Target Genes of *miR-122*

Gene Symbol	Human			Mouse			Molecular Function	No. Binding Sites
	T3/T1	Sc-H	MFE-H	an/c	Sc-H	MFE-M		
NUMBL	3.1	181	−20.5	4.5	131	−14.5	Protein binding	8
FOXJ3	1.6	176	−21	1.7	133	−10.6	Transcription factor	6
XPO6	2.2	174	−22.3	1.7	125	−16.4	Nuclear protein transport	2
SLC7A1	2.6	173	−22.4	1.7	173	−23.6	Amino acid transport	16
STX6	1.6	169	−20.9	2.5	135	−17.2	Protein transport	5
AP3M2	1.6	168	−19.9	3.0	129	−15.9	Protein trafficking	3
G6PC3	2.1	167	−18.4	6.1	158	−13.1	Glucose-6-phosphatase	1
GALNT10	1.6	167	−20.4	1.9	152	−20.5	Calcium binding	8
RIPK5	1.8	166	−18	1.6	150	−16.6	Kinase activity	4
TPD52L2	3.0	166	−23.8	16.3	140	−16.5	Cell proliferation	11
AKT3	2.0	165	−18.7	2.1	162	−15.6	Cell proliferation, apoptosis	3
FUNDC2	2.5	165	−18	2.1	161	−15.8	HCV core binding protein	4
MAPK11	3.2	165	−20.2	1.6	123	−19.1	MAPK activity	2
ALS2CR13	2.0	162	−17.3	6.7	163	−17	Unknown	7
BACH2	1.8	162	−15	2.7	140	−13.5	Transcription factor	11
ATP11A	2.0	161	−12.9	1.9	162	−18.1	Transport ions	9
SORT1	2.2	161	−16.2	2.0	154	−15.3	Cell differentiation	7
ATP1A2	3.5	160	−17	1.5	132	−11.7	Ion concentration balance	7
ADAM17	1.7	159	−19	2.0	122	−17	Cell cell interaction	1
DUSP2	1.8	159	−13.4	1.6	123	−11.1	MAPK phosphatase	2
OSMR	2.5	159	−15.8	2.9	142	−15.5	Cell proliferation	4
RABIF	1.7	159	−20.1	2.4	139	−15.1	Small GPT regulator activity	2
PALM	2.3	156	−15.9	16.1	161	−18.7	Cell mobility and cell shape	3
SPRED1	2.2	156	−21.2	1.6	145	−19.8	Activate MAPK kinase	1
AACS	1.8	155	−13.8	1.8	163	−17.8	Isoprenoid biogenesis	2
TBX19	2.1	155	−17.2	4.3	131	−13.1	Transcription factor	5
UBAP2	2.2	155	−18.8	2.7	131	−23.3	Ubiquitin associated protein	2
EGLN3	3.9	154	−17	1.6	137	−15.7	Apoptosis	1
NCAM1	1.9	154	−15.2	3.8	154	−15.2	Cell differentiation	4
MECP2	2.2	153	−12.1	3.1	160	−26.2	Transcription	18
CS	1.6	152	−12.6	1.8	148	−11.9	Catalyzes citrate synthesis	3
FOXP1	1.6	152	−10.8	1.8	167	−17.7	Transcription factor	7
RAB11FIP1	1.5	152	−20.1	1.9	133	−13.3	Protein transport	5
RAB6B	1.5	152	−13.3	1.6	164	−19.6	GTPase	13
TRIB1	2.1	152	−17.4	1.8	134	−12.8	Kinase activity	4
TTYH3	1.8	152	−17.1	1.9	160	−16.6	Chloride anion channel	5
ALDOA	3.7	151	−13.2	2.2	157	−16.7	Amino acid transport	2
ANXA11	2.0	151	−18.6	4.3	139	−17.2	Calcium binding	11
CLDN18	1.7	151	−18.5	1.9	130	−15.1	Cell and cell adhesion	4
ENTPD4	2.0	151	−18.5	2.0	131	−13.5	Calcium binding	3
NFATC2IP	2.7	151	−19.9	2.2	135	−15.2	Protein modification	4
ANK2	2.1	150	−12	3.1	137	−17.9	Cell proliferation	5
MEP1A	4.3	150	−17.8	1.6	132	−12.8	Peptidase	3
NFATC1	1.8	150	−13.1	2.3	148	−14.9	Transcription factor	6
SLC7A11	9.5	150	−19.5	1.6	164	−14.4	Amino acid transport	4

The relative gene expression level detected by microarray assay is shown as the mean ratios of T3/T1 for HCC samples and an/c for mice treated with antagomiR-122 (an) compared to the control mm-antagomiR122 (c). The criteria used for target selection are the prediction score of "seed match" (Sc) and minimum free energy (MFE). Scores for the human and mouse genes are labeled as Sc-H and Sc-M, respectively. MFE values for the human and mouse genes are labeled as MFE-H and MFE-M, respectively. Gene information is provided with Gene Symbol and Molecular Function. "No. Binding Sites" indicates number of putative *miR-122* binding sites in the 3′UTR region of the putative target genes. Positions of the predicted binding sites are listed in Supporting Table 3.

triphosphatases.[35] Whether the restoration of *miR-122* or the knockdown of ADAM17 disturbed the equilibrium of the Rho–guanosine triphosphatases remains to be elucidated.

Overexpression of miR-122 or Knockdown of ADAM17 Suppresses In Situ Tumor Formation and Metastasis. To determine whether *miR-122* and its target gene are associated with tumorgenesis or metastasis, Mahlavu cells were infected with shLuc, *miR-122*, or shADAM17 lentiviruses and implanted by either the subcutaneous route into the flanks of nude mice or orthotopically into the livers of nude mice. Restoration of *miR-122* or silencing of ADAM17 significantly suppressed overall tumor growth, as assessed by tumor volume (Fig. 6A). Moreover, the orthotopic tumor model yielded a similar tumor growth trend in the original injection site. ShLuc-

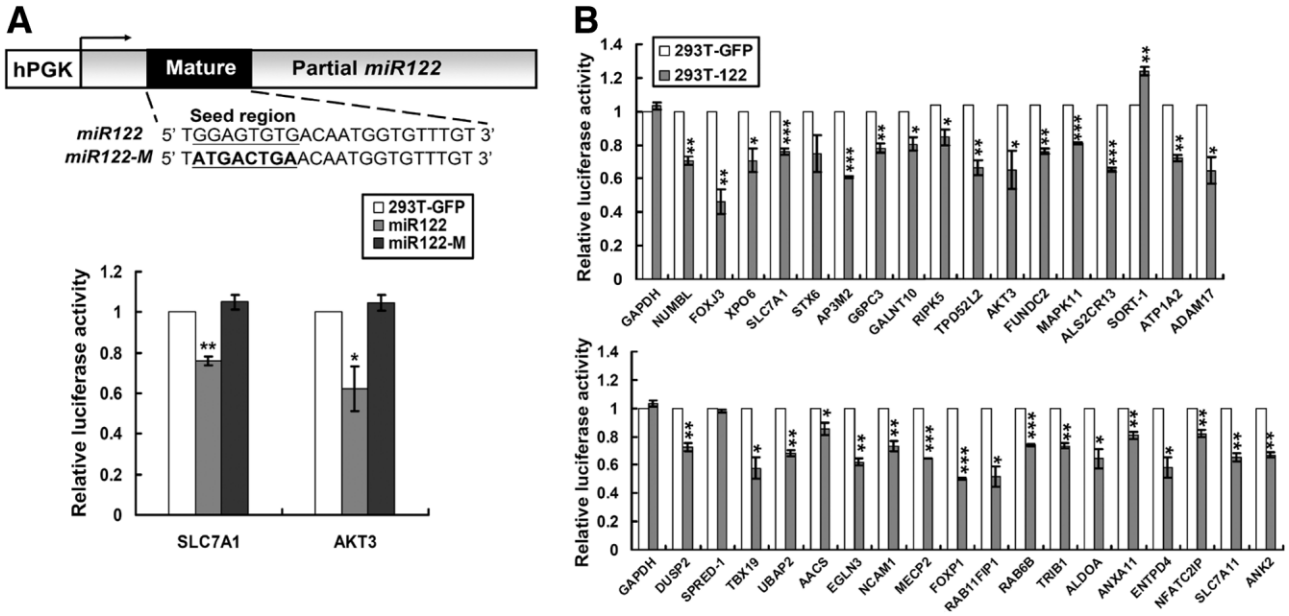

Fig. 3. Confirmation of *miR-122* target genes. (A) Diagram depicting the 3′UTR reporter assay. The *miR-122* mutant (*miR-122M*) has the seed region mutated (upper panel). The specificity of the reporter assay was examined with parental *miR-122* and *miR122-M* targeting the reporters for SLC7A1 and AKT3 (lower panel). The 3′UTR reporter assay was carried out in 293T cells overexpressing *miR-122* or *miR122-M*. Lenti-GFP served as the negative control (293T-GFP). Cells were cotransfected with the pGL3-3′UTR construct and pRL-TK vector (Promega) using jetPEI. Luciferase assays were performed 48 hours after transfection using the Dual-Luciferase Reporter Assay System (Promega). Firefly luciferase activity was normalized to Renilla luciferase activity. The effect of *miR-122* was expressed relative to the average value from cells infected with the lenti-GFP viruses. (B) Overall, 32 of the 35 3′UTR constructs demonstrated a significant reduction in luciferase activity for 293T cells overexpressing *miR-122* (293T-122).

infected Mahlavu cells showed extensive hepatic invasion with a larger tumor volume; this contrasts with single smaller tumor focus that was found in the *miR-122* and shADAM17 groups (Fig. 6B,C). The tumor growth reduction and metastasis shutdown may be speculated to be the results of angiogenesis inhibition. To confirm this speculation, subcutaneous and orthotopic tumors were subjected to neoangiogenesis analysis by staining with anti-CD31 antibody (Fig. 6D). Quantitative analysis showed that there was significant reductions in the blood vessels present in the *miR-122* and shADAM17 groups compared to shLuc control for the subcutaneous tumors (Fig. 6E, left panel) and for the orthotopic tumors (Fig. 6E, right panel). Thus, *miR-122* would seem to regulate tumorigenesis and intrahepatic metastasis via angiogenesis inhibition at least in part through its target ADAM17.

Discussion

Recent work has started to shed light on the importance of miRNA in hepatocarcinogensis. Deregulation of liver-specific *miR-122* and a linkage to liver diseases has attracted intense interest; nonetheless, experimental affirmation of its role in liver pathology is lacking. In this study, we demonstrated that *miR-122* acts as a tumor suppressor gene for hepatocarcinogenesis, particularly intrahepatic metastasis. Restoration of *miR-122* has some impact on the epithelial-mesenchymal transition as shown by reduction in vimentin, a mesenchymal marker (Fig. 5B). Related to this, reduced *in vitro* cell migration and invasion, *in vivo* tumor growth, and local invasion can be detected upon restoration of *miR-122*. We are intrigued to find that restoration of *miR-122* in highly migratory HCC cells neither triggered apoptosis nor inhibited *in vitro* cell proliferation (Supporting Fig. 1); instead, it led to a significant inhibition of angiogenesis (Fig. 6D,E).

Similar to a classical transcription factor, microRNAs exert their activity via regulation of their target genes. We report here 32 direct target genes of *miR-122*. This is the first time that 32 empirically verified target genes have been discovered in a single study. We attributed our success in target prediction to several tactics. First, in accordance with the consensus of posttranscriptional suppression by miRNAs, we correlated expression of *miR-122* with its candidate targets from two microarray datasets constructed from mouse and human livers known to be low in endogenous *miR-122* (Table 1). This complies with the species conservation principle and, as a result, greater confidence can be given to each target gene identified. Second, the use of both a high miRanda score

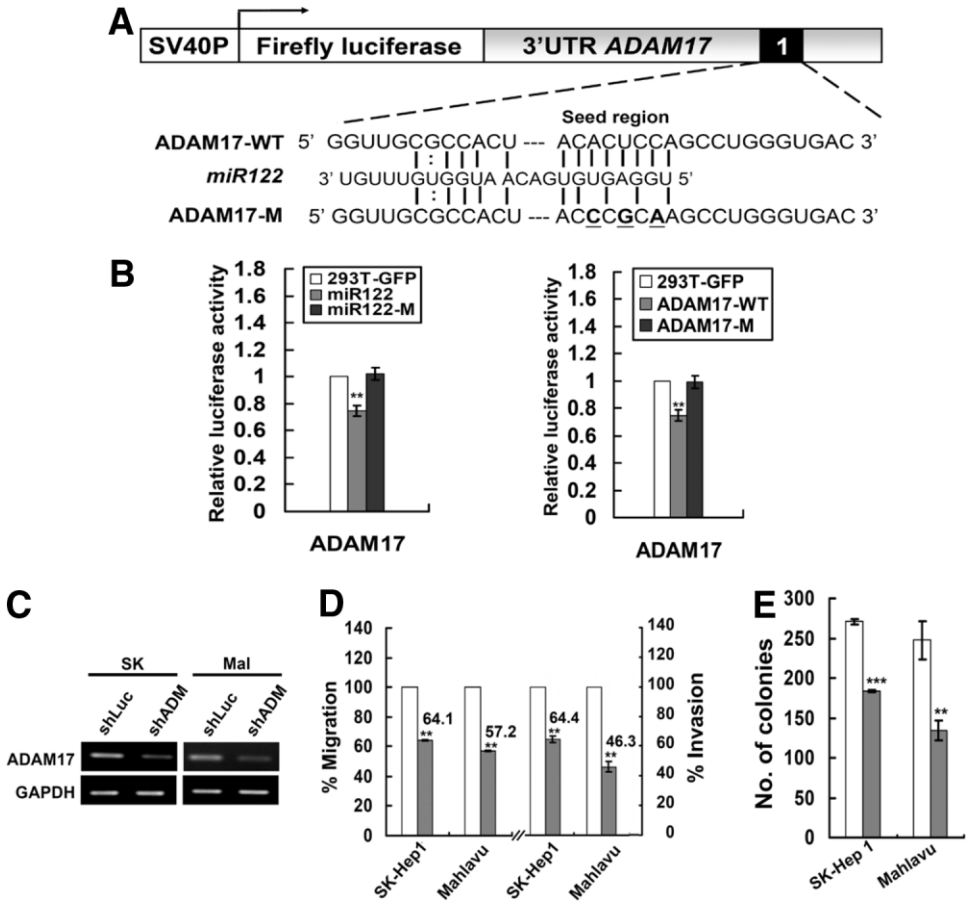

Fig. 4. ADAM17 is a *miR-122* target and regulates the transforming activities of HCC cells. (A) Diagram showing the *miR-122* binding site mutant of *ADAM17*. (B) Verification of the binding site specificity. Reduction of luciferase activity driven by ADAM17-3′UTR construct was observed in cells expressing wild-type *miR-122* (293T-122) but not in cells overexpressing mutant *miR-122* (293T-122M) (left panel). Reporter constructs containing *ADAM17-M* failed to suppress the luciferase activity (right panel). (C) Suppression of *ADAM17* mRNA expression by RNA interference. ADAM17 knockdown resulted in a reduction in (D) cell migration (left panel) and invasion (right panel) activity as well as (E) anchorage-independent growth in soft agar in two HCC cell lines. Cells were infected with either control shLuc (white bar) or shADAM17 (gray bar) for 24 hours, which was followed by 2-day puromycin (2 μg/mL) selection before the cells were plated for the migration, invasion assays, or soft-agar assay. Data are an average of triplicates for each condition. $^{**}P < 0.01$; $^{***}P < 0.001$.

and low miRanda minimum free energy was able to pinpoint most probable targets.[36,37] Finally, the false-positives from the prediction were eliminated by differential validation using both a wild-type and a "seed region" mutant of *miR-122* via the 3′UTR reporter assay (Fig. 3B, Supporting Tables 4 and 5).

This set of 32 target genes is unique among those reported to-date. Lack of concordance may be attributed to several variables. The sources of liver tissues, either normal livers in which *miR-122* was acutely depleted by an antisense approach or cancerous livers in which there is protracted down-regulation of *miR-122* that has occurred naturally,[12,21] are likely to present different target gene pools. Many of the most affected genes from the studies using a loss-of-function approach involved hepatic lipid metabolism.[4,17,38] In contrast, the molecular functions of the *miR-122* targets presented here are affiliated with transcription regulation, amino acid transport, protein trafficking, and cell signaling (Table 1, Supporting Fig. 3). To unravel the biological role of *miR-122* in HCC metastasis, ADAM17 was identified as a critical downstream target. Knockdown of ADAM17 in migratory HCC cells suppressed the *in vitro* proliferation, migration, invasion, and anchorage-independent growth of these HCC cells (Fig. 4D,E); this was in addition to suppressing *in vivo* tumor growth, angiogenesis, and local invasion in the liver *milieu* (Fig. 6). The collective results from RNA interference substantiate that *ADAM17* is a *bona fide* oncogene involved in liver cancer. Up-regulation of *ADAM17* has been detected in a wide variety of human cancers including HCC[28,32,33] and colorectal liver metastasis.[39] ADAM17 facilitates cleavage-activation of TNFα[40] and selected ligands of EGF receptor (EGFR)[41] as well as modulating integrin signaling during cell adhe-

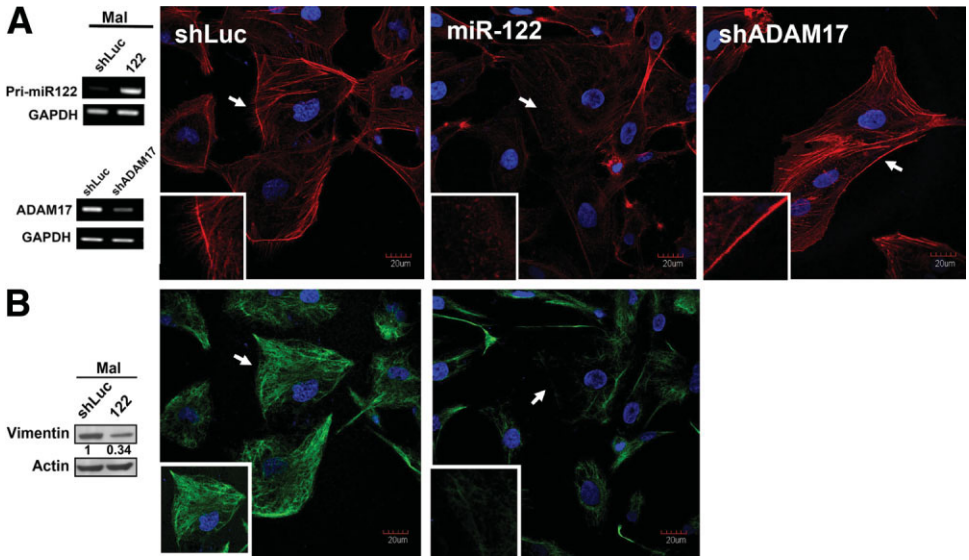

Fig. 5. Restoration of *miR-122* or suppression of ADAM17 expression affected the cytoskeleton of HCC cells. (A) Loss of actin filament was found in *miR-122*–overexpressing Malhlavu cells (*miR-122*), while a severe reduction in membrane protrusions was observed after ADAM17 knockdown (shADAM17). Inset: higher magnification view of the F-actin and the membrane protrusions. *MiR-122* overexpression and ADAM17-knockdown were confirmed by RT-PCR (left panel). (B) Restoration of *miR-122* resulted in differential expression of vimentin. As shown by western blot (left) and immunofluorescence (right), a significant loss of vimentin was detected upon *miR-122* expression. shADAM17 did not affect expression of vimentin. Images were taken 5-7 days after infection. Cells were fixed and stained with rhodamine-phalloidin, DAPI (4′,6-diamidino-2-phenylindole), or anti-vimentin to detect F-actin, the nucleus, and vimentin, respectively. Bar, 20 μm. Original magnification: 60×.

sion and migration.[42,43] In addition, coexpression of activated EGFR and ADAM17 has been observed in the neoplastic and endothelial cells from colon cancers,[44] suggesting a role in angiogenesis. We postulate that ADAM17 is a likely component of the tumor stroma that facilitates angiogenesis and tissue remodeling during HCC progression. Further studies in these areas will be required.

We also noticed that the outcome of ADAM17 knockdown is reminiscent of the restoration of *miR-122*, both *in vitro* and *in vivo*, but that ADAM17 knockdown shows a stronger intensity; this may be explained because the net effect of *miR-122* restoration represents an overall response from all target genes. MicroRNAs are pivotal modulators of gene expression and yet their involvement as effectors of cell signaling is largely unknown and is a matter of intense study at present. Our preliminary results showed that restoration of *miR-122* greatly reduces activation of focal adhesion kinase (FAK), v-raf-1 murine leukemia viral oncogene homolog (Raf), mitogen-activated protein kinase(MEK), and extracellular-signal-regulated kinase (ERK) (Supporting Fig. 6). This finding provides clues as to how *miR-122*–mediated alteration of actin cytoskeleton occurs, but leaves open the question as to whether the expression of *miR-122* controls hepatocyte differentiation. ADAM17 is probably not the only target of *miR-122* that is relevant to tumorigenesis and metastasis. Identification of forkhead box P1[13] and SRY (sex determining region Y)-box 4[23] (unpublished data), two transcription factors known to regulate hepatocarcinogenesis and HCC metastasis, as the direct targets of *miR-122*, suggests a coordinated regulatory program involving miRNA and transcription factors during liver carcinogenesis. The input of the other targets needs to be evaluated in order to fully understand how *miR-122* controls metastasis.

In summary, we have identified a *miR-122*–ADAM17 link that is a novel constituent in hepatocarcinogenesis. Recently, it has been shown by Zhou et al. that a selective inhibitor of ADAM17 effectively prevents activation of multiple EGFR ligands and suppresses resistance to the EGFR inhibitor gefitinib in non–small cell lung cancer.[31] Moreover, amphiregulin, a preferred substrate of the ADAM17 sheddase, has been shown to contribute to the transformed phenotype of HCC cells[33]; thus, ADAM17 is a potential modulator of HCC cell proliferation. It will be necessary to gain a better understanding of whether *miR-122* overexpression disrupts EGFR signaling by way of ADAM17 modulation. Although the efficacy of EGFR-targeted chemotherapies in HCC is less than satisfactory,[45] restoration of *miR-122* might have more far-reaching effects. With the concomitant down-regulation of its targets, including ADAM17, a rational therapeutic strategy based on *miR-122* may be beneficial to patients with HCC.

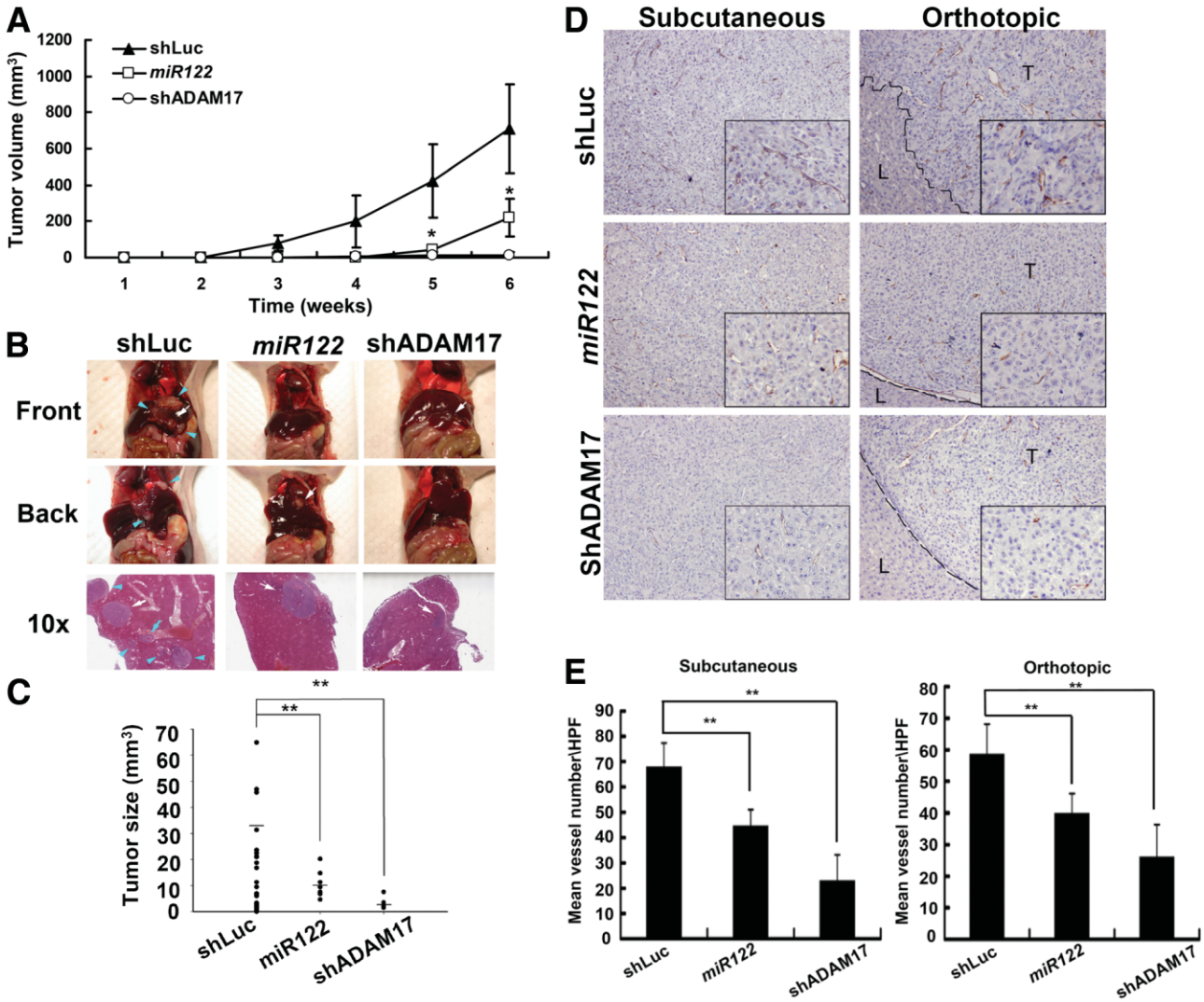

Fig. 6. Effects of *miR-122* overexpression or ADAM17-knockdown on subcutaneous tumors and orthotopic liver tumors. (A) *In vivo* subcutaneous tumor growth curves of shLuc-infected, *miR-122*-infected, or shADAM17-infected Mahlavu cells (n = 7). *$P < 0.05$. (B) Gross morphology of representative livers and abdominal cavity organs (upper and middle panels) as well as hematoxylin and eosin–stained images of representative tumors (lower panel) after intrahepatic injection of shLuc-infected, *miR-122*-infected, or shADAM17-infected Mahlavu cells. The liver tumors were examined 7 weeks after cell injection. The shLuc-infected Mahlavu cells showed extensive hepatic invasion, whereas only one tumor focus was found in the *miR-122* and shADAM17 groups. The panels showed the morphology of the tumors from the injected site (white arrows) and the disseminating tumors (blue arrowheads) in the abdominal cavity in the shLuc group. It is important to note the presence of the tumor cells invading the hepatic vessels and forming small metastatic focus (blue arrow, shLuc). No metastatic tumors were found in the *miR-122* group or in the shADAM17 group. Original magnification: 100×. (C) The graph shows the volumes and numbers of orthotopic and metastatic tumor foci in the livers after injecting shLuc-infected, *miR-122*-infected, or shADAM17-infected Mahlavu cells (n = 7, 31 tumor foci in shLuc group, seven foci in *miR-122* group, and three foci in shADAM17 group). The lines show the average tumor sizes. Note that there are significant reductions in the tumor sizes when the experiment is carried out with *miR-122*-infected or shADAM17-infected Mahlavu cells compared to the shLuc control. The average volumes of the original orthotopic and metastatic tumors of the shLuc-treated group are significantly higher than those of the *miR-122* and shADAM17-treated groups (35.5 ± 17.2 versus 10.7 ± 5.3 and 3.8 ± 2.6 mm^3, respectively; $P < 0.01$). (**$P < 0.01$). (D) Blood vessel distributions of the subcutaneous and orthotopic tumors as revealed by immunohistochemistry staining using CD31 antibody. The left panel shows the vessel distributions in the subcutaneous tumors caused by shLuc-infected, *miR-122*-infected, and shADAM17-infected Mahlavu cells. Right panel shows the vessel distributions in the orthotopic tumors. The dotted lines show the edges of normal liver area (L) and tumor area (T). Note that the shLuc tumor has invasive edges while the *miR-122* and shADAM17 tumors show smooth edges. The black frame indicates a representative 400× magnification field. The original magnification is 200×. (E) Bar chart shows comparisons of the mean CD31-positive vessel number per high-power field of the various tumor sections. Significant reductions in the number of CD31-positive blood vessels was found for the *miR-122* and shADAM17 groups compared to shLuc control group when the subcutaneous tumors were examined (n = 20, 44.5 ± 6.5, 22.8 ± 10.5 versus 67.7 ± 9.7, $P < 0.01$, left panel). Similar results were found for the orthotopic tumors (n = 20, 39.7 ± 10.5, 26.0 ± 6.0 versus 58.5 ± 9.8, right panel). **$P < 0.01$.

Acknowledgment: We thank Drs. C. K. Chou and W. C. Lin for their invaluable comments, the Microarray and Gene Expression Analysis Core Facility of the VGH National Yang-Ming University Genome Research Center (VYMGC) for their technical support and the National RNAi Core Facility for providing the RNAi reagents.

References

1. Lee RC, Feinbaum RL, Ambros V. The C. elegans heterochronic gene lin-4 encodes small RNAs with antisense complementarity to lin-14. Cell 1993;75:843-854.
2. Reinhart BJ, Slack FJ, Basson M, Pasquinelli AE, Bettinger JC, Rougvie AE, et al. The 21-nucleotide let-7 RNA regulates developmental timing in Caenorhabditis elegans. Nature 2000;403:901-906.
3. Bagga S, Bracht J, Hunter S, Massirer K, Holtz J, Eachus R, et al. Regulation by let-7 and lin-4 miRNAs results in target mRNA degradation. Cell 2005;122:553-563.
4. Krutzfeldt J, Rajewsky N, Braich R, Rajeev KG, Tuschl T, Manoharan M, et al. Silencing of microRNAs in vivo with 'antagomirs'. Nature 2005;438:685-689.
5. Lim LP, Lau NC, Garrett-Engele P, Grimson A, Schelter JM, Castle J, et al. Microarray analysis shows that some microRNAs downregulate large numbers of target mRNAs. Nature 2005;433:769-773.
6. Calin GA, Dumitru CD, Shimizu M, Bichi R, Zupo S, Noch E, et al. Frequent deletions and down-regulation of micro- RNA genes miR15 and miR16 at 13q14 in chronic lymphocytic leukemia. Proc Natl Acad Sci U S A 2002;99:15524-15529.
7. He L, Thomson JM, Hemann MT, Hernando-Monge E, Mu D, Goodson S, et al. A microRNA polycistron as a potential human oncogene. Nature 2005;435:828-833.
8. El-Serag HB, Rudolph KL. Hepatocellular carcinoma: epidemiology and molecular carcinogenesis. Gastroenterology 2007;132:2557-2576.
9. Okabe H, Satoh S, Kato T, Kitahara O, Yanagawa R, Yamaoka Y, et al. Genome-wide analysis of gene expression in human hepatocellular carcinomas using cDNA microarray: identification of genes involved in viral carcinogenesis and tumor progression. Cancer Res 2001;61:2129-2137.
10. Cheung ST, Chen X, Guan XY, Wong SY, Tai LS, Ng IO, et al. Identify metastasis-associated genes in hepatocellular carcinoma through clonality delineation for multinodular tumor. Cancer Res 2002;62:4711-4721.
11. Murakami Y, Yasuda T, Saigo K, Urashima T, Toyoda H, Okanoue T, et al. Comprehensive analysis of microRNA expression patterns in hepatocellular carcinoma and non-tumorous tissues. Oncogene 2006;25:2537-2545.
12. Budhu A, Jia HL, Forgues M, Liu CG, Goldstein D, Lam A, et al. Identification of metastasis-related microRNAs in hepatocellular carcinoma. HEPATOLOGY 2008;47:897-907.
13. Datta J, Kutay H, Nasser MW, Nuovo GJ, Wang B, Majumder S, et al. Methylation mediated silencing of MicroRNA-1 gene and its role in hepatocellular carcinogenesis. Cancer Res 2008;68:5049-5058.
14. Varnholt H. The role of microRNAs in primary liver cancer. Ann Hepatol 2008;7:104-113.
15. Liang Y, Ridzon D, Wong L, Chen C. Characterization of microRNA expression profiles in normal human tissues. BMC Genomics 2007;8:166.
16. Chen JF, Mandel EM, Thomson JM, Wu Q, Callis TE, Hammond SM, et al. The role of microRNA-1 and microRNA-133 in skeletal muscle proliferation and differentiation. Nat Genet 2006;38:228-233.
17. Esau C, Davis S, Murray SF, Yu XX, Pandey SK, Pear M, et al. miR-122 regulation of lipid metabolism revealed by in vivo antisense targeting. Cell Metab 2006;3:87-98.
18. Jopling CL, Yi M, Lancaster AM, Lemon SM, Sarnow P. Modulation of hepatitis C virus RNA abundance by a liver-specific MicroRNA. Science 2005;309:1577-1581.
19. Lin CJ, Gong HY, Tseng HC, Wang WL, Wu JL. miR-122 targets an anti-apoptotic gene, Bcl-w, in human hepatocellular carcinoma cell lines. Biochem Biophys Res Commun 2008;375:315-320.
20. Chang J, Nicolas E, Marks D, Sander C, Lerro A, Buendia MA, et al. miR-122, a mammalian liver-specific microRNA, is processed from hcr mRNA and may downregulate the high affinity cationic amino acid transporter CAT-1. RNA Biol 2004;1:106-113.
21. Kutay H, Bai S, Datta J, Motiwala T, Pogribny I, Frankel W, et al. Downregulation of miR-122 in the rodent and human hepatocellular carcinomas. J Cell Biochem 2006;99:671-678.
22. Gramantieri L, Ferracin M, Fornari F, Veronese A, Sabbioni S, Liu CG, et al. Cyclin G1 is a target of miR-122a, a microRNA frequently downregulated in human hepatocellular carcinoma. Cancer Res 2007;67:6092-6099.
23. Liao YL, Sun YM, Chau GY, Chau YP, Lai TC, Wang JL, et al. Identification of SOX4 target genes using phylogenetic footprinting-based prediction from expression microarrays suggests that overexpression of SOX4 potentiates metastasis in hepatocellular carcinoma. Oncogene 2008;27:5578-5589.
24. John B, Enright AJ, Aravin A, Tuschl T, Sander C, Marks DS. Human MicroRNA targets. PLoS Biol 2004;2:e363.
25. Birney E, Andrews D, Caccamo M, Chen Y, Clarke L, Coates G, et al. Ensembl 2006. Nucleic Acids Res 2006;34:D556-D561.
26. Lewis BP, Shih IH, Jones-Rhoades MW, Bartel DP, Burge CB. Prediction of mammalian microRNA targets. Cell 2003;115:787-798.
27. Lu YS, Kashida Y, Kulp SK, Wang YC, Wang D, Hung JH, et al. Efficacy of a novel histone deacetylase inhibitor in murine models of hepatocellular carcinoma. HEPATOLOGY 2007;46:1119-1130.
28. Mochizuki S, Okada Y. ADAMs in cancer cell proliferation and progression. Cancer Sci 2007;98:621-628.
29. McGowan PM, Ryan BM, Hill AD, McDermott E, O'Higgins N, Duffy MJ. ADAM-17 expression in breast cancer correlates with variables of tumor progression. Clin Cancer Res 2007;13:2335-2343.
30. Zheng X, Jiang F, Katakowski M, Kalkanis SN, Hong X, Zhang X, et al. Inhibition of ADAM17 reduces hypoxia-induced brain tumor cell invasiveness. Cancer Sci 2007;98:674-684.
31. Zhou BB, Peyton M, He B, Liu C, Girard L, Caudler E, et al. Targeting ADAM-mediated ligand cleavage to inhibit HER3 and EGFR pathways in non-small cell lung cancer. Cancer Cell 2006;10:39-50.
32. Ding X, Yang LY, Huang GW, Wang W, Lu WQ. ADAM17 mRNA expression and pathological features of hepatocellular carcinoma. World J Gastroenterol 2004;10:2735-2739.
33. Castillo J, Erroba E, Perugorria MJ, Santamaria M, Lee DC, Prieto J, et al. Amphiregulin contributes to the transformed phenotype of human hepatocellular carcinoma cells. Cancer Res 2006;66:6129-6138.
34. Dong JM, Leung T, Manser E, Lim L. cAMP-induced morphological changes are counteracted by the activated RhoA small GTPase and the Rho kinase ROKalpha. J Biol Chem 1998;273:22554-22562.
35. Ladwein M, Rottner K. On the Rho'd: the regulation of membrane protrusions by Rho-GTPases. FEBS Lett 2008;582:2066-2074.
36. Hsu PW, Huang HD, Hsu SD, Lin LZ, Tsou AP, Tseng CP, et al. miRNAMap: genomic maps of microRNA genes and their target genes in mammalian genomes. Nucleic Acids Res 2006;34:D135-D139.
37. Rajewsky N. microRNA target predictions in animals. Nat Genet 2006;38(Suppl):S8-S13.
38. Elmen J, Lindow M, Silahtaroglu A, Bak M, Christensen M, Lind-Thomsen A, et al. Antagonism of microRNA-122 in mice by systemically administered LNA-antimiR leads to up-regulation of a large set of predicted target mRNAs in the liver. Nucleic Acids Res 2008;36:1153-1162.
39. Lin HM, Chatterjee A, Lin YH, Anjomshoaa A, Fukuzawa R, McCall JL, et al. Genome wide expression profiling identifies genes associated with colorectal liver metastasis. Oncol Rep 2007;17:1541-1549.

40. Black RA, Rauch CT, Kozlosky CJ, Peschon JJ, Slack JL, Wolfson MF, et al. A metalloproteinase disintegrin that releases tumour-necrosis factor-alpha from cells. Nature 1997;385:729-733.
41. Borrell-Pages M, Rojo F, Albanell J, Baselga J, Arribas J. TACE is required for the activation of the EGFR by TGF-alpha in tumors. EMBO J 2003; 22:1114-1124.
42. Bax DV, Messent AJ, Tart J, van Hoang M, Kott J, Maciewicz RA, et al. Integrin alpha5beta1 and ADAM-17 interact in vitro and co-localize in migrating HeLa cells. J Biol Chem 2004;279:22377-22386.
43. Huang J, Bridges LC, White JM. Selective modulation of integrin-mediated cell migration by distinct ADAM family members. Mol Biol Cell 2005;16:4982-4991.
44. Blanchot-Jossic F, Jarry A, Masson D, Bach-Ngohou K, Paineau J, Denis MG, et al. Up-regulated expression of ADAM17 in human colon carcinoma: co-expression with EGFR in neoplastic and endothelial cells. J Pathol 2005;207:156-163.
45. Furuse J. Growth factors as therapeutic targets in HCC. Crit Rev Oncol Hematol 2008;67:8-15.